applied sciences

MDPI

Article

# Impact of Osteotomy in Surgically Assisted Rapid Maxillary Expansion Using Tooth-Borne Appliance on the Formation of Stresses and Displacement Patterns in the Facial Skeleton—A Study Using Finite Element Analysis (FEA)

**Ewa Zawiślak [1,*], Anna Olejnik [1], Roman Frątczak [2] and Rafał Nowak [1]**

1 Department of Maxillofacial Surgery, Wroclaw Medical University, Borowska 213, 50-556 Wrocław, Poland; anna.olejnik@umed.wroc.pl (A.O.); rafal.nowak@umed.wroc.pl (R.N.)
2 NOBO Solutions S.A., Al. Kasztanowa 3A-5, 53-125 Wrocław, Poland; roman.fratczak@nobosolutions.com
* Correspondence: ewazawislak0@op.pl; Tel.: +48-71-734-36-00

Received: 4 November 2020; Accepted: 19 November 2020; Published: 21 November 2020

check for updates

**Abstract:** The analysis aimed at studying stresses reduced according to Huber's hypothesis and displacement patterns at selected sites of the facial skeleton using a tooth-borne appliance in surgically assisted rapid maxillary expansion. Five different variants of osteotomy of the midface and a variant without surgical intervention were compared to determine the best model for making an incision in the maxilla. The finite element analysis (FEA) was used for the study. Five osteotomy variants and a variant without osteotomy were modelled using a tooth-borne appliance on a facial skeleton model of a 23-year-old woman with skeletal malocclusion. The finite element mesh was constructed based on the geometry imported into the ANSYS 15.0 (Swanson Analysis System of USA) software, in which calculations were performed using the finite element analysis. Stress distributions and displacement patterns along the X, Y and Z axes are presented for each osteotomy variant with the expansion of the tooth-borne appliance at a level of 0.5 mm. As a result of the analysis it was found that osteotomy of the palatal suture in conjunction with Le Fort I osteotomy has the biggest impact on the course of maxillary expansion. If no osteotomy is performed, an increase in stresses reduced according to Huber occurs in the entire facial skeleton with a simultaneous absence of maxillary expansion.

**Keywords:** finite elements analysis; SARPE; maxillary constriction; maxillary expansion; orthognathic surgery

## 1. Introduction

Maxillary constriction is a frequent disorder in the structure of the facial skeleton [1–4]. The occurrence of the disorder in the entire population is estimated at 9.4%. Almost 30% of orthodontically treated adult patients are affected by this abnormality in which half of the lower dental arch overlaps the upper arch [1,5]. Complete crossbite occurs in 13–24% of the European children population, 7% in American and less than 1–2% in African children [6].

A popular method for treating this disorder is rapid maxillary expansion using various appliances as sources of force [7–10]. The treatment aims at obtaining optimal values of the width of the anterior and posterior upper dental arch, which leads to stable and functional occlusion [11,12] as well as improves respiratory functions [13,14]. Maspero et al. [15] suggest that rapid maxillary expansion in growing patients with maxillary hypoplasia may support proper condylar growth and facial symmetry. Orthodontic, orthodontic and surgical, as well as surgical methods are used in the treatment of crossbite.

The type of therapy used for expanding the palatal suture should be strictly dependent on the patient's age [1,8–10]. The elasticity of the facial skeleton and the possibility of orthopaedic operation to expand the bone base of the maxilla decreases with age. According to various authors [3,5] the upper age limit for orthodontic treatment is 14–18 years. As regards the time of closing the craniofacial sutures and a possibility for performing orthodontic operations, sexual dimorphism is taken into account by some researchers. Baumrind and Korn report that the closure of maxillary bone sutures occurs at the age of 14–15 in women and 15–16 in men [16].

The first reports on the subject of palatal expansion using an orthodontic method come from the first half of the 19th century. Talma and Lefulon reported on palatal expansion using a C-shaped spring device [17]. In 1860, Angell expanded the maxilla in a 14-year-old girl, and his report was described in the periodical "Dental Cosmos" [18]. After bone growth is complete, osteotomy is required at sites of increased bone resistance in the midface. In adult patients, an orthodontic expansion therapy only results in deflection of the alveolar process of the maxilla, with little or no orthopaedic effect [19,20]. The SARME (surgically assisted rapid maxillary expansion) therapy is the method of choice. As a result of the complex structure and mechanics of the facial skeleton numerous patterns of osteotomy and corticotomy of the midface were developed. The precursor of surgically assisted rapid palatal expansion (SARPE) was probably Brown, who in 1938 described osteotomy of the palatal suture combined with fixing an appliance for maxillary expansion [17,20]. The first osteotomies in SARME were performed only to the palatal suture. The types of osteotomies evolved in the following years. Isaacson and Ingram believe that the palatal suture is not the only bone resistance site for proper maxillary expansion in the SARME therapy [21]. Timms et al. are of the opinion that only the palatal suture requires incision, thus conditioning maxillary expansion in adult patients [20]. To date, no consensus has been reached on how to perform osteotomy of the midface using methods of surgically assisted rapid maxillary expansion [20].

The purpose of the following analysis is to present stress distributions and displacement patterns of specific structures in the area of the facial skeleton in surgically assisted rapid maxillary expansion therapy using a tooth-borne appliance. By comparing five different osteotomy variants and one without surgical intervention, the best model for making an incision in the maxilla will be determined. Five types of osteotomy of the midface and expansion of the appliance at a level of 0.5 mm were modelled using the finite element analysis.

## 2. Materials and Methods

The finite elements method (FEM) or finite elements analysis (FEA) is a numerical method for solving partial differential mechanical equations in two or three space variables. It has had a monumental impact on virtually all areas of engineering, biomechanics and applied science. From the viewpoint of approximation theory, the method provides a systematic approach to piecewise approximation over subdomains that produces sequences of functions that can approximate arbitrary members of, say, Sobolev spaces, arbitrarily closely in appropriate norms.

To solve a problem, the FEM subdivides a large system into smaller, simpler parts that are called finite elements. Each element is assigned a material property to represent the physical properties of the model.

The main difficulty with the FEM approach is the construction of the complicated 3-dimensional (3D) shape of the craniofacial complex and its tissues and assigned them with adequate material property.

When the model is prepared, boundary conditions are set, and forces are applied to simulate applied investigated loads. The response is then calculated and visualized to analyze and discuss.

### *2.1. Construction of the Facial Skeleton Model for the Finite Element Analysis*

The geometric model of the facial skeleton was built based on CT scans of a 32-year-old woman, a generally healthy patient, with skeletal malocclusion. In the Slicer3D program (Slicer 4.10.2) the bone structures of the patient's facial skeleton were separated. The separation was made by determining attenuation thresholds corresponding to the bone structure. CT scan voxels with attenuation in that range formed a volumetric model of the patient's facial skeleton (Figure 1)

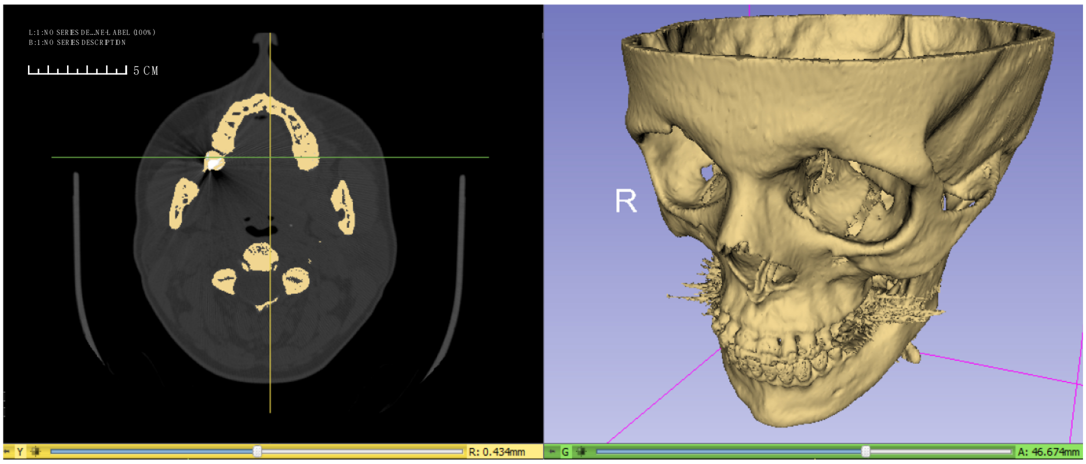


**Figure 1.** Computer tomography (CT) parallel scan slice with a separate three-dimensional finite element model of craniofacial skeleton of 32-year-old women with skeletal malocclusion (Slicer 4.10.2®).

The separated structures were then exported for further processing in the form of a surface mesh in the stereolithography (stl) format. Mesh errors resulting from the limited resolution of scans and low contrast of certain areas were fixed in Blender (Blender 2.82a®). As a result, a high quality surface mesh was obtained. The surface mesh was exported in the stl format to the GMSH program (GMSH 4.1.®), where a resulting volumetric mesh of 10 nodal tetrahedrons of the second order was created. The finite element mesh was imported into the ANSYS 15.0 (Swanson Analysis System of USA) software, where material properties were assigned according to Pekhale et al. (Table 1), boundary conditions were determined and calculations using the finite element analysis were performed [22]. The result is a dense mesh of higher order finite elements ensuring accurate mapping of the stress distribution and displacement field. The discreet model consisted of over 1.8 million elements whose edges were 1–2 mm in length. Figure 2 shows the orientation of the system of coordinates for the model.

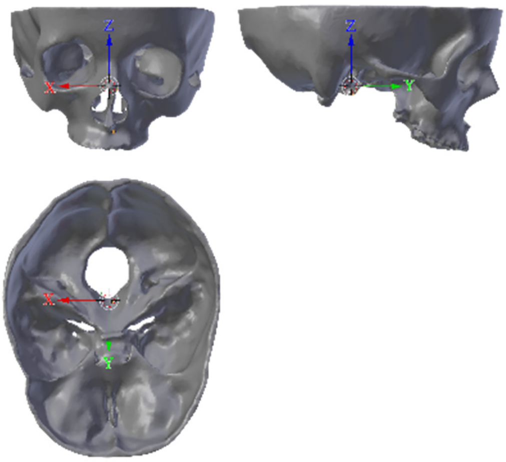


**Figure 2.** The model of craniofacial skeleton used for finite element analysis and orientation of the system of coordinates on the model. The foramen magnum, which formed the base of the model, was constrained in its displacement by the X, Y, and Z direction.

**Table 1.** The mechanical properties of the components of the finite element model constructed for the present study.

| Variable | Young's Modulus [MPa] | Poisson's Ratio |
|---|---|---|
| Compact bone | 13,700 | 0.26 |
| Cancellous bone | 1370 | 0.3 |
| Enamel | 80,000 | 0.26 |
| Dentin | 20,000 | 0.15 |
| Stainless steel | 200,000 | 0.3 |

### *2.2. Construction of the Orthodontic Appliance*

A tooth-borne orthodontic appliance was modelled using beam-shaped finite elements of circular cross-section. The diameter of 3.5 mm was set for the wire in the arms of the appliance, and 3.0 mm for the central part. The dental appliance was modelled using steel for its material. The appliance was fixed onto teeth 4, 5 and 6. The expansion of the central part of the appliance by 0.5 mm was modelled by assigning to its central part of 9.62 mm in length an artificial coefficient of thermal expansion with a value of $5.197 \times 10^{-4}$ and raising its temperature by 100 °C. The design of the modelled appliance is shown in Figure 3. The facial skeleton model was fixed at 5 points around the circumference of the foramen magnum.

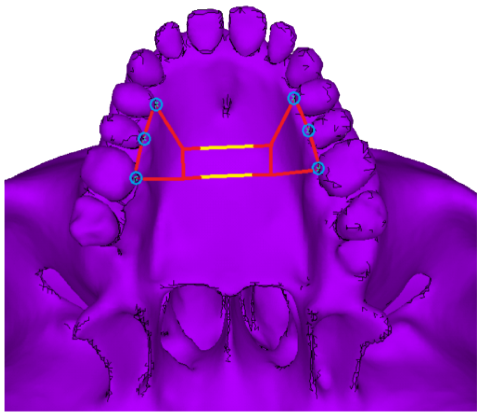

**Figure 3.** Schematic representation of the orthodontic appliance fixed to the teeth—tooth borne type. The module expanded by 0.5 mm is marked in yellow. Fixing onto the teeth of the facial skeleton is marked with blue markings.

### *2.3. Types of Osteotomy on the Model of the Facial Skeleton*

By using dense discretization, the facial skeleton models were created with five osteotomy variants and one without osteotomy and an orthodontic appliance with a central module expansion of 0.5 mm. In total, 6 numerical models were analyzed. They are shown in Figure 4, where the course of the osteotomy line is demonstrated schematically. Osteotomy of the palatal suture is marked in red. Le Fort I osteotomy without separation from the pterygoid processes of the sphenoid bone is marked in yellow, and with separation from the sphenoid bone is marked in blue. A detailed description of the scope of modelled osteotomies and the order of the maps of stresses reduced according to Huber and presented in the figures are shown in Table 2.

**Table 2.** A detailed course of modelled osteotomies and the order of the maps of stresses reduced according to Huber presented in the figures.

| | |
|---|---|
| Model 1—the model used for finite element analysis—without osteotomy | Model 2—the model used for finite element analysis—sagittal osteotomy |
| Model 3—the model used for finite element analysis—transversal osteotomy modo Le Fort I without PMJ separation | Model 4—the model used for finite element analysis—transversal osteotomy modo Le Fort I with PMJ separation |
| Model 5—the model used for finite element analysis—sagittal osteotomy with transversal osteotomy modo Le Fort I without PMJ separation | Model 6—the model used for finite element analysis—sagittal osteotomy with transversal osteotomy modo Le Fort I with PMJ separation |

PMJ—pterygomaxillary junction.

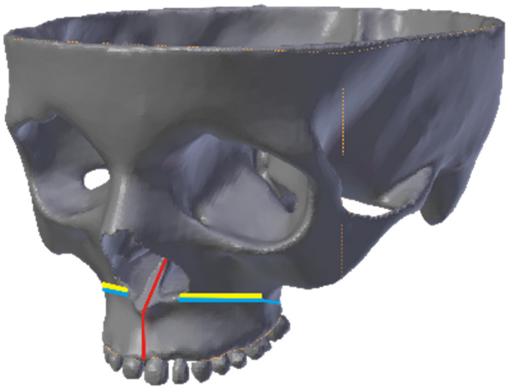

**Figure 4.** Schematic representation of the osteotomy line on the 3D finite element model of facial skeleton. Red color marked-sagittal osteotomy; yellow color marked-transversal osteotomy modo Le Fort I without pterygomaxillary junction separation; blue color marked—transversal osteotomy modo Le Fort I with pterygomaxillary junction separation.

The stress reduced according to Huber's hypothesis was determined for selected anatomical structures of the facial skeleton. In addition, the distribution of reduced stresses is shown using colored contour stripes corresponding to the stress level at a given site in Figure 5A–F and Figure 6A–F in front and bottom views in the order shown in Table 2.

The displacement in mm along the X, Y, Z axes was determined for selected anatomical structures of the facial skeleton.

The displacement along the X axis corresponded to changes in the buccolingual direction. Positive values describe displacement in the buccal direction, and negative in the lingual direction.

The displacement along the Y axis corresponded to changes in the anterior-posterior direction. Positive values describe displacement in the anterior direction, and negative in the posterior direction.

The displacement along the Z axis corresponded to changes in the superior-inferior direction. Positive values describe displacement in the superior direction, and negative in the inferior direction.

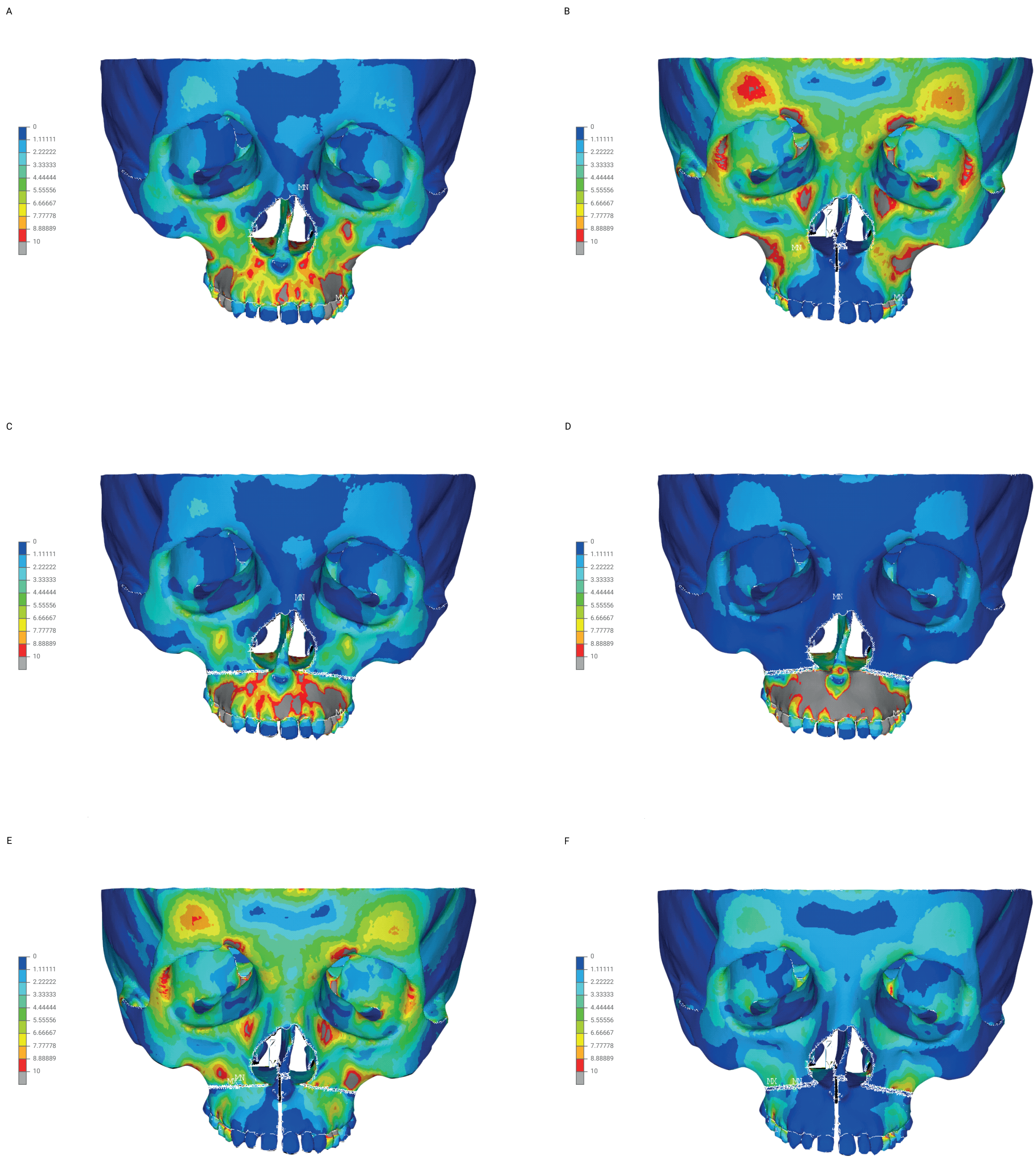


**Figure 5.** (**A**–**F**). The finite element model showing according to Huber stress distribution over craniofacial skeleton—front view (scale 0–10 MPa) caused by palatal expansion using five different surgical procedures and without osteotomy: (**A**) without osteotomy; (**B**) sagittal osteotomy; (**C**) transversal osteotomy modo Le Fort I without PMJ separation; (**D**). transversal osteotomy modo Le Fort I with PMJ separation; (**E**) sagittal osteotomy with transversal osteotomy modo Le Fort I without PMJ separation; (**F**) the model used for finite element analysis—sagittal osteotomy with transversal osteotomy modo Le Fort I with PMJ separation. PMJ—pterygomaxillary junction.

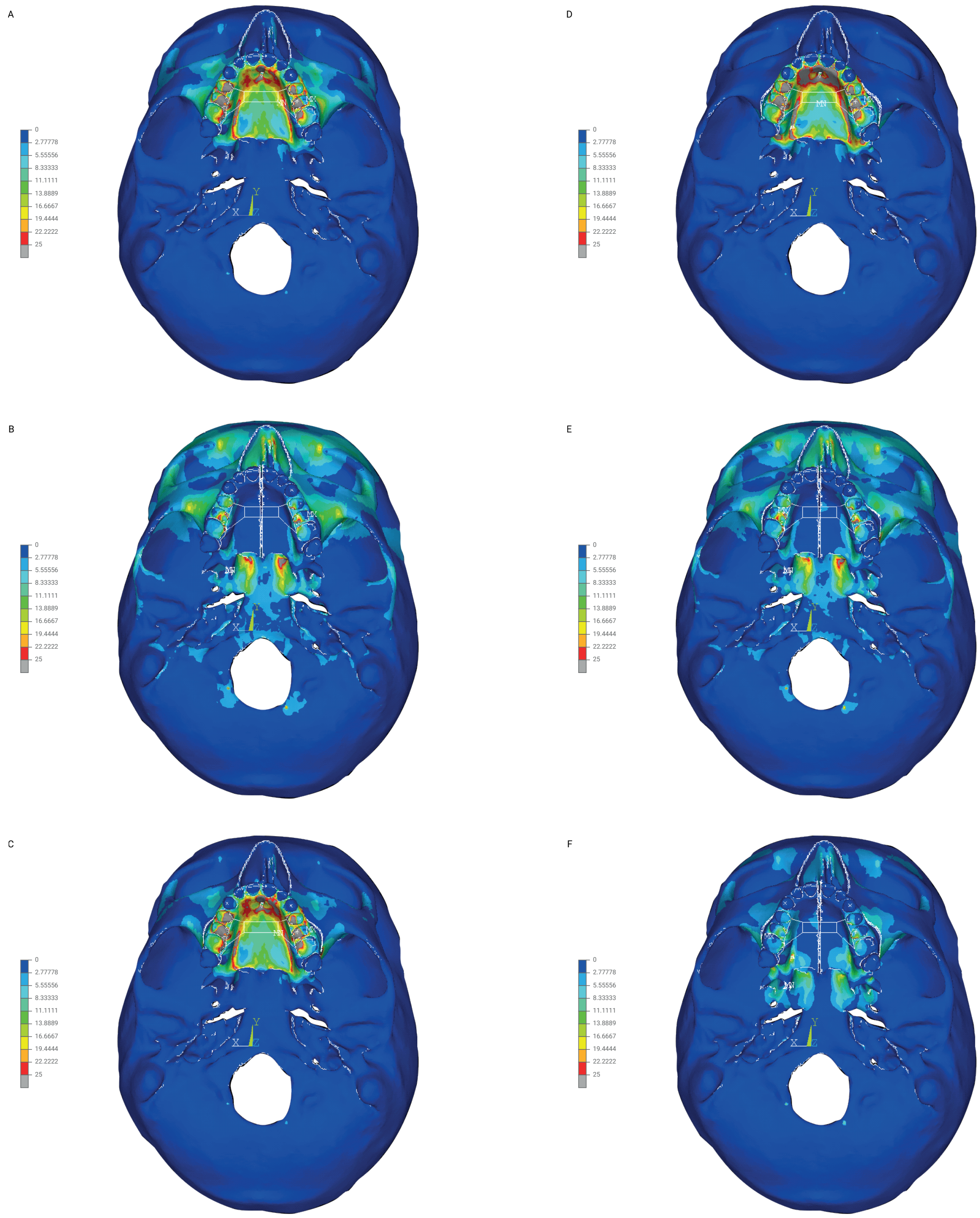


**Figure 6.** (**A**–**F**). The finite element model showing according to Huber stress distribution over craniofacial skeleton—bottom view (scale 0–25 MPa) caused by palatal expansion using five different surgical procedures and without osteotomy: (**A**) without osteotomy; (**B**) sagittal osteotomy; (**C**) transversal osteotomy modo Le Fort I without PMJ separation; (**D**) transversal osteotomy modo Le Fort I with PMJ separation; (**E**) sagittal osteotomy with transversal osteotomy modo Le Fort I without PMJ separation; (**F**) the model used for finite element analysis—sagittal osteotomy with transversal osteotomy modo Le Fort I with PMJ separation. PMJ—pterygomaxillary junction.

## 3. Results

### *3.1. Stress Reduced According to Huber (MPa)*

The highest values of stress reduced according to Huber in various parts of the facial skeleton were recorded for the model without osteotomy (model 1), for the model with Le Fort I osteotomy (model 3) and for the model with Le Fort I osteotomy and separation in PMJ (model 4). The highest stress values (>10 MPa) were found on the anterior walls of the maxillary sinus (model 1), for the alveolar process in the region of all dental groups (models 1, 3 and 4) and in the anterior region of the hard palate (models 1, 3 and 4). Particularly noteworthy is the unfavorable stress redistribution (>10 MPa) below the osteotomy line on model 4, where Le Fort I osteotomy with separation in PMJ was performed (Figure 5D).

On model 2, stress values for the alveolar process range from 0 to 7.7 MPa, on model 5 from 0 to 7.7 MPa, and on model 6 from 0 to 2.2 MPa. On the hard palate, osteotomy of the palatal region reduced stresses to a level of 1.1 MPa in the anterior and posterior region of the hard palate (models 2, 5, 6). On models 1, 3 and 4 without palatal osteotomy, stress values in the anterior part were at a level of >25 MPa, and in the posterior part the value was 13.3 PMa.

Detailed analysis results and the distribution of stress reduced according to Huber in various regions of the facial skeleton are presented in Table 3 and Figure 5A–F and Figure 6A–F.

**Table 3.** Stress distribution according to Huber on the craniofacial model (MPa) with various surgical procedures and tooth born orthodontic appliance using finite element analysis.

| Anatomical Structures | Model I No Surgery | Model II | Model III | Model IV | Model V | Model VI |
|---|---|---|---|---|---|---|
| Nasofrontal suture | 2.2 | 5.5 | 1.1 | 1.1 | 4.4 | 2.2 |
| Zygomaticomaxillary suture | 3.3 | 5.5 | 4.4 | 1.1 | 4.4 | 2.2 |
| Arcus superciliaris—brow ridge | 2.2 | 8.8 | 2.2 | 2.2 | 7.7 | 3.3 |
| Zygomaticofrontal suture | 4.4 | 7.7 | 3.3 | 2.2 | 7.7 | 3.3 |
| Palatal suture anterior region | >25 | 1.1 | >25 | >25 | 1.1 | 1.1 |
| Palatal suture posterior region | 13.8 | 1.1 | 13.8 | 13.8 | 1.1 | 1.1 |
| Supraorbital margin | 2.2 | 4.4 | 2.2 | 1.1 | 4.4 | 2.2 |
| Infraorbital margin | 4.4 | 5.5 | 2.2 | 1.1 | 7.7 | 2.2 |
| Apertura piriformis—the lowest point | 5.5 | 1.1 | >10 | >10 | 1.1 | 1.1 |
| Anterior wall of maxillary sinus | >10 | 4.4 | 7.7 | 1.1 | 3.3 | 2.2 |
| Zygomaticoalveolar crest | >10 | >10 | 5.5 | 3.3 | 5.5 | 3.3 |
| Processus alveolaris of maxillae regio incisors and canine | 7.7 | 1.1 | 10 | >10 | 1.1 | 1.1 |
| Processus alveolaris of maxillae regio premolars | >10 | 8.8 | >10 | >10 | 7.7 | 3.3 |
| Processus alveolaris of maxillae regio molars | 5.5 | 1.1 | 5.5 | 7.7 | 3.3 | 3.3 |
| Crown/collum fifth maxilla tooth | >10 | 5.5 | >10 | >10 | 5.5 | 4.4 |

### *3.2. Displacements of Selected Facial Skeleton Structures along the X, Y, Z Axes (mm)*

The smallest displacement along the X axis in the buccal direction was found on the facial skeleton model without osteotomy (model 1), on the model with Le Fort I osteotomy (model 3) and on the model with Le Fort I osteotomy and separation from the pterygoid process (model 4). Displacements on the above-mentioned models were in the 0.04–0.13 mm range. On the models with palatal incision, displacements along the X axis in the buccal direction ranged from 0.22 to 0.31 mm on model 2, from 0.22 to 0.31 mm on model 5, and from 0.22 to 0.4 mm on model 6. The largest displacement in the buccal direction was found at the mesial incisal angle of the central maxillary incisor (0.4 mm) on model 6 of the facial skeleton.

On the model without osteotomy (model 1) displacements ranged from −0.05 to 0.1 mm along the Y axis. On model 2 they ranged from 0.05 to 0.03 mm, on model 3 from −0.5 to 0.03 mm, on model 4 from −0.05 to 0.05 mm, on model 5 from 0.03 to 0.05 mm, and on model 6 from −0.01 to 0.07 mm.

The largest displacement in the anterior direction was found at the mesial incisal angle of the central maxillary incisor (0.07 mm) on model 6 of the facial skeleton.

On the model without osteotomy, displacements ranged from −0.03 to 0.1 mm along the Z axis. On model 2, they ranged from 0.01 to 1.0 mm, on model 3 from −0.01 to 0.03 mm, on model 4 from −0.03 to 0.07 mm, on model 5 from −0.05 to 0.07 mm, and on model 6 from −0.05 to 0.07 mm. The largest displacement in the superior direction was found on the posterolateral surface of the maxilla (1.0 mm) on model 2 of the facial skeleton.

Detailed displacement values (mm) along the X, Y, Z axes at selected sites of the facial skeleton are shown in Table 4.

**Table 4.** Displacement values of selected anatomical structures (mm) along the X, Y, Z, with various surgical procedures and tooth born orthodontic appliance using finite element analysis.

| | Variable | Model I | Model II | Model III | Model IV | Model V | Model VI |
|---|---|---|---|---|---|---|---|
| X | Mesial incisal angle of maxillary tooth 1 | +0.04 | +0.31 | +0.04 | +0.04 | +0.31 | +0.4 |
| | Buccal cusp tip of maxillary tooth 5 | +0.04 | +0.22 | +0.04 | +0.13 | +0.31 | +0.31 |
| | Posterolateral surface of the maxilla | +0.04 | +0.22 | +0.04 | +0.04 | +0.22 | +0.22 |
| | Apertura piriformis—the lowest point | +0.04 | +0.22 | +0.04 | +0.04 | +0.22 | +0.22 |
| Y | Mesial incisal angle of maxillary tooth 1 | −0.05 | +0.05 | −0.5 | −0.5 | +0.05 | +0.07 |
| | Buccal cusp tip of maxillary tooth 5 | +0.01 | +0.03 | +0.01 | +0.03 | +0.03 | +0.01 |
| | Posterolateral surface of the maxilla | +0.01 | +0.03 | +0.03 | +0.05 | +0.03 | −0.01 |
| | Apertura piriformis—the lowest point | −0.03 | +0.03 | −0.03 | −0.03 | +0.03 | +0.05 |
| Z | Mesial incisal angle of maxillary tooth 1 | −0.03 | +0.01 | −0.03 | −0.03 | −0.05 | −0.05 |
| | Buccal cusp tip of maxillary tooth 5 | −0.03 | +0.07 | +0.01 | +0.03 | +0.07 | +0.05 |
| | Posterolateral surface of the maxilla | +0.03 | +0.07 | +0.03 | +0.07 | +0.07 | +0.07 |
| | Apertura piriformis—the lowest point | −0.03 | +0.01 | −0.03 | −0.03 | −0.05 | −0.05 |

X—buccolingual; (+)—buccal, (−)—lingual; Y—anterioposterior (front-back); (+)—anterior, (−)—posterior; Z—superioinferior (upper part-lower part); (+)—superior, (−)—inferior.

## 4. Discussion

The surgically assisted rapid maxillary expansion therapy is successful when optimal widths of the upper dental arch are achieved. The increase in transverse dimensions should be skeletal, not dental, which determines stability in the treatment of the disorder [23,24]. After bone growth is complete, it is necessary to perform surgical procedures to release the bone resistance sites in the midface region and therefore allow for maxillary expansion [13,17]. The anatomical structure of the maxilla is reinforced by the apertura piriformis (anterior reinforcement), zygomaticoalveolar crest (lateral reinforcement) and pterygopalatine suture (posterior reinforcement). The reinforcements begin at the base of the maxillary alveolar process and run vertically, bending around the orbital rim down to the base of the skull [25,26]. Le Fort I osteotomy with separation of all bone junctions around the maxilla and sagittal osteotomy without separation of the nasal septum is proposed by Mommaerts [13]. The inventor of the method of surgically assisted maxillary expansion using a bone-borne appliance (TPD—transpalatal distraction) declares that this method of expansion has good effects.

The finite element analysis is a good simulation for evaluating surgical procedures performed on the facial skeleton in the method of surgically assisted rapid maxillary expansion [27,28]. It allows one to evaluate complex stress distributions and displacement patterns on the facial skeleton model [29]. Interpretation of the results of the analysis should be made carefully and prudently, because it is a skeletal model created on the basis of a 3D computed tomography reconstruction of the facial skeleton with material properties assigned according to Pekhale et al. [22].

Currently, in the literature, there is no agreement as to the scope of osteotomy in surgically assisted rapid maxillary expansion [17,20,30,31]. What method should be chosen? It seems that the therapeutic team's experience and the surgeon's preferences are of great importance in this regard [17]. The authors' study presents six variants of the approach to the subject of surgically assisted maxillary expansion.

The analysis performed by the authors points out significant differences in the distribution of stresses reduced according to Huber as well as displacement patterns for the modelled variants of osteotomies.

No osteotomy performed (model 1) generates stresses >10 MPa in the palatal suture, anterior maxillary sinus wall, zygomaticoalveolar crest and the teeth, to which the appliance is fixed. The displacements in the buccolingual direction (X axis) for all measuring points were 0.04 mm. According to our analysis no increase occurred in the transverse dimensions of the midface. The results of the study correlate with work of numerous authors in the field of maxillary expansion [1,6,13,32]. The absence of osteotomy generates stresses with no maxillary expansion, which may lead to uncontrolled fractures and pain in the patient. [33]. Handelman et al. present a different opinion. The authors report on an effective maxillary expansion therapy received by 47 adult patients, with no use of surgical procedures [34].

Osteotomy of the palatal suture (model 2) decreases stresses, according to Huber, down to 1.1 MPa in the hard palate and the alveolar process of the maxilla in the incisal region. An increase in stress also occurs in the arcus supercilliaris region up to a maximum of 10 MPa. An increase in transverse dimensions (displacements along the X axis) in the variants with palatal osteotomy ranges from 0.22 to 0.4 mm. It seems that, in order to increase lateral dimensions of the maxilla, osteotomy of the palatal suture produces a satisfactory effect with a moderate increase in stress in the facial skeleton.

Maxillary incision only along the Le Fort I line (models 3 and 4) results in unfavorable redistribution of stress reduced according to Huber to the region below the osteotomy line. The analysis showed stresses >10 MPa around the entire region of the maxillary alveolar process, on lowest point of the apertura piriformis and the anterior and posterior region of the hard palate. Increases in transverse dimensions (displacement along the X axis) are minimal and range from 0.04 to 0.13 mm. This gives no grounds for performing an independent Le Fort I osteotomy and Le Fort I osteotomy with separation in PMJ. Practically, no displacement along the X axis occurs when stresses exceed 10 MPa. Furthermore, the incisors are displaced in the posterior direction at a level of 0.5 mm, which is undesirable.

The combination of Le Fort I osteotomy with an incision in the palatal suture without separation in PMJ (model 5) results in a favorable decrease in stress, according to Huber, below the osteotomy line according to the Le Fort I line to maximum values of 7.7 MPa. In addition, a significant reduction in stress occurs on the teeth to which the appliance is fixed to a level of 4.4 MPa. This is of great significance for possible periodontological effects of the teeth to which the appliance is fixed [1,13,17]. Increases in transverse dimensions (displacement along the X axis) range from 0.22 to 0.31 mm for selected structures specified in Table 4. The expansion in relation to the anterior and lateral teeth is the same and is 0.31 mm. What occurs is parallel expansion.

The combination of Le Fort I osteotomy with an incision in the palatal suture and separation in PMJ (model 6) gives a significant reduction in stress in the orbital regions and the entire midface to values of 4.4 MPa maximally. According to our analysis, separation in PMJ decreases stresses reduced according to Huber from >10 MPa to 7.7 MPa of the maximum values in the entire facial skeleton. In the literature, there is no unambiguous position of the authors regarding separation of the maxilla from the pterygoid process of the sphenoid bone [17]. The proponents of full maxillary separation argue that it positively affects the extent of expansion of the maxilla and ensures adequate rotation of its fragments [35–39]. Matteini and Mommaerts point out the need for full osteotomy if performance of posterior distraction and planned parallel extension of the maxillary fragments are intended [13,40]. The finite element analyses (FEA) support the idea of releasing all bone resistance sites in the maxilla before its expansion is attempted. Holberg et al. describe the risk of stresses and uncontrolled fractures of the facial skeleton without osteotomy of the maxilla when an attempt to expand it is made after bone growth is complete [29,41,42]. Separation from the pterygoid processes of the sphenoid bone increases the risk of surgical complications, such as descending palatal artery haemorrhage or pterygoplexus haemorrhage as well as osteonecrosis of the maxilla [17,31,43]. According to Carvallo et al., the absence of total maxillary separation results in an increased incidence of orthodontic complications (22.99% vs.

9.79%, $p < 0.001$) with asymmetrical or incorrect expansion [44]. This issue is worth to note espiecially in time of COVID-19 pandemic when access to orthodontic care is limited [45].

Increases in transverse dimensions on model 6 (displacement along the X axis) range from 0.22 to 0.4 mm for selected structures specified in Table 4. Expansion in relation to the anterior and lateral teeth is not the same. Greater expansion occurs in the anterior region of the maxilla.

## 5. Conclusions

To expand the maxilla, it is necessary to perform surgically assisted rapid maxillary expansion after bone growth is complete. From a mechanical point of view, the highest bone resistance includes midpalate suture, maxillary buttresses and pterygomaxillary junction. According to the results of our analysis, cutting of those areas provides stress reduction in the facial skeleton during maxillary expansion.

This means that sagittal osteotomy of the midpalatal suture with transversal osteotomy modo Le Fort I with or without PMJ separation should be the most sufficient surgical method during maxillary expansion.

The choice of osteotomy should be determined by a reduction in postsurgical complications in the patient. The experience of the treatment team as well as the degree and shape of maxillary constriction seems crucial in choosing the type of osteotomy performed.

**Author Contributions:** Conceptualization: R.N., E.Z. and R.F.; methodology: E.Z., R.F. and A.O.; software: R.F. and E.Z.; validation: R.F. and R.N.; formal analysis: R.F., R.N. and E.Z.; investigation: R.F. and A.O.; resources: R.N. and E.Z.; data curation R.N., E.Z. and A.O.; writing—original draft preparation: E.Z. and A.O. writing—review and editing: E.Z., A.O. and R.N.; visualization: E.Z. and R.N.; supervision: R.N., E.Z. and A.O.; project administration: E.Z., R.N. and R.F. All authors have read and agreed to the published version of the manuscript.

**Funding:** This research received no external funding.

**Conflicts of Interest:** The authors declare no conflict of interest.

## References

1. Verstraaten, J.; Kuijpers-Jagtman, A.M.; Mommaerts, M.Y.; Bergé, S.J.; Nada, R.M.; Schols, J.G. A systematic review of the effects of bone-borne surgical assisted rapid maxillary expansion. *J. Cranio Maxillofac. Surg.* **2010**, *38*, 166–174. [CrossRef] [PubMed]
2. Bailey, L.J.; White, R.P.; Proffit, W.R.; Turvey, T.A. Segmantal LeFort I osteotomy for management of transverse maxillary deficiency. *J. Oral Maxillofac. Surg.* **1997**, *55*, 728–731. [CrossRef]
3. Erdinç, A.E.; Ugur, T.; Erbay, E. A comparison of different treatment techniques for posterior crossbite in the mixed dentition. *Am. J. Orthod. Dentofac. Orthop.* **1999**, *116*, 287–300. [CrossRef]
4. Lee, K.-J.; Park, Y.-C.; Park, J.-Y.; Hwang, W.-S. Miniscrew-assisted nonsurgical palatal expansion before orthognathic surgery for a patient with severe mandibular prognathism. *Am. J. Orthod. Dentofac. Orthop.* **2010**, *137*, 830–839. [CrossRef] [PubMed]
5. Marshall, S.D.; Shroff, B. Long-term Skeletal Changes with Rapid Maxillary Expansion: A Review of the Literature. *Semin. Orthod.* **2012**, *18*, 128–133. [CrossRef]
6. Chamberland, S.; Proffit, W.R. Short-term and long-term stability of surgically assisted rapid palatal expansion revisited. *Am. J. Orthod. Dentofac. Orthop.* **2011**, *139*, 815–822.e1. [CrossRef]
7. Laptook, T. Conductive hearing loss and rapid maxillary expansion. *Am. J. Orthod.* **1981**, *80*, 325–331. [CrossRef]
8. Haas, A.J. Palatal expansion: Just the beginning of dentofacial orthopedics. *Am. J. Orthod.* **1970**, *57*, 219–255. [CrossRef]
9. Bishara, S.; Staley, R.N. Maxillary expansion: Clinical implications. *Am. J. Orthod. Dentofac. Orthop.* **1987**, *91*, 3–14. [CrossRef]
10. Proffit, W.R.; Turvey, T.A.; Phillips, C. Orthognathic surgery: A hierarchy of stability. *Int. J. Adult Orthod. Orthognath. Surg.* **1996**, *11*, 191–204.
11. Northway, W.; Meade, J.B. Surgically assisted rapid maxillary expansion: A comparison of technique, response, and stability. *Angle Orthod.* **1997**, *67*, 20.

12. Koo, Y.-J.; Choi, S.-H.; Keum, B.-T.; Yu, H.-S.; Hwang, C.-J.; Melsen, B.; Lee, K.-J. Maxillomandibular arch width differences at estimated centers of resistance: Comparison between normal occlusion and skeletal Class III malocclusion. *Korean, J. Orthod.* **2017**, *47*, 167–175. [CrossRef] [PubMed]
13. Abate, A.; Cavagnetto, D.; Fama, A.; Matarese, M.; Lucarelli, D.; Assandri, F. Short term effects of rapid maxillary expansion on breathing function assessed with spirometry: A case-control study. *Saudi Dent. J.* **2020**. [CrossRef]
14. Lanteri, V.; Farronato, M.; Ugolini, A.; Cossellu, G.; Gaffuri, F.; Parisi, F.M.R.; Cavagnetto, D.; Abate, A.; Maspero, C. Volumetric Changes in the Upper Airways after Rapid and Slow Maxillary Expansion in Growing Patients: A Case-Control Study. *Materials* **2020**, *13*, 2239. [CrossRef] [PubMed]
15. Maspero, C.; Cavagnetto, D.; Abate, A.; Cressoni, P.; Farronato, M. Effects on the Facial Growth of Rapid Palatal Expansion in Growing Patients Affected by Juvenile Idiopathic Arthritis with Monolateral Involvement of the Temporomandibular Joints: A Case-Control Study on Posteroanterior and Lateral Cephalograms. *J. Clin. Med.* **2020**, *9*, 1159. [CrossRef] [PubMed]
16. Korn, E.; Baumrind, S. Transverse Development of the Human Jaws Between the Ages of 8.5 and 15.5 Years, Studied Longitudinally With Use of Implants. *J. Dent. Res.* **1990**, *69*, 1298–1306. [CrossRef]
17. Koudstaal, M.J.; Poort, L.; Van Der Wal, K.; Wolvius, E.; Prahl-Andersen, B.; Schulten, A. Surgically assisted rapid maxillary expansion (SARME): A review of the literature. *Int. J. Oral Maxillofac. Surg.* **2005**, *34*, 709–714. [CrossRef]
18. M'Quillen, J.H. Review of Dental Literature and Art. *Dental Cosmos* **1860**, *1*, 535–540.
19. Betts, N.J.; Vanarsdall, R.L.; Barber, H.D.; Higgins-Barber, K.; Fonseca, R.J. Diagnosis and treatment of transverse maxillary deficiency. *Int. J. Adult Orthod. Orthognath. Surg.* **1995**, *10*, 75–96.
20. Chrcanovic, B.R.; Custódio, A.L.N. Orthodontic or surgically assisted rapid maxillary expansion. *Oral Maxillofac. Surg.* **2009**, *13*, 123–137. [CrossRef]
21. Isaacson, R.J.; Ingram, A.H. Forces produced by rapid maxillary expansion, II. Forces present during treatment. *Angle Orthod.* **1964**, *34*, 261–270. [CrossRef]
22. Pekhale, N.; Maheshwari, A.; Kumar, M.; Kerudi, V.V.; Patil, H.; Patil, B. Evaluation of stress patterns on maxillary posterior segment when intruded with mini implant anchorage: A three-dimensional finite element study. *APOS Trends Orthod.* **2016**, *6*, 18–23. [CrossRef]
23. Marchetti, C.; Pironi, M.; Bianchi, A.; Musci, A. Surgically assisted rapid palatal expansion vs. segmental Le Fort I osteotomy: Transverse stability over a 2-year period. *J. Cranio Maxillofac. Surg.* **2009**, *37*, 74–78. [CrossRef] [PubMed]
24. Seeberger, R.; Gander, E.; Hoffmann, J.; Engel, M. Surgical management of cross-bites in orthognathic surgery: Surgically assisted rapid maxillary expansion (SARME) versus two-piece maxilla. *J. Cranio Maxillofac. Surg.* **2015**, *43*, 1109–1112. [CrossRef] [PubMed]
25. Sicher, H. *Oral Anatomy*; CV Mosby: St. Louis, MO, USA, 1963.
26. Pollock, R.A. *Craniomaxillofacial Buttresses. Anatomy and Operative Repair*; Thieme Medical Publishers, Inc.: New York, NY, USA, 2012.
27. Işeri, H.; Tekkaya, A.E.; Bilgiç, Ö.S. Biomechanical effects of rapid maxillary expansion on the craniofacial skeleton, studied by the finite element method. *Eur. J. Orthod.* **1998**, *20*, 347–356. [CrossRef]
28. Jafari, A.; Shetty, K.; Kumar, M. Study on stress distribution and displacement of various craniofacial structures following application of transverse orthopedic forces—A three-dimensional FEM study. *Angle Orthod.* **2003**, *73*, 12–20. [CrossRef]
29. Holberg, M.D.M.D.C. Effects of Rapid Maxillary Expansion on the Cranial Base—An FEM-Analysis. *J. Orofac. Orthop. Fortschr. Kieferorthop.* **2005**, *66*, 54–66. [CrossRef]
30. Silverstein, K.; Quinn, P.D. Surgically-assisted rapid palatal expansion for management of transverse maxillary deficiency. *J. Oral Maxillofac. Surg.* **1997**, *55*, 725–727. [CrossRef]
31. Sangsari, A.H.; Sadr-Eshkevari, P.; Al-Dam, A.; Friedrich, R.E.; Freymiller, E.; Rashad, A. Surgically Assisted Rapid Palatomaxillary Expansion with or without Pterygomaxillary Disjunction: A Systematic Review and Meta-Analysis. *J. Oral Maxillofac. Surg.* **2016**, *74*, 338–348. [CrossRef]
32. Günbay, T.; Akay, M.C.; Günbay, S.; Aras, A.; Koyuncu, B.Ö.; Sezer, B. Transpalatal Distraction Using Bone-Borne Distractor: Clinical Observations and Dental and Skeletal Changes. *J. Oral Maxillofac. Surg.* **2008**, *66*, 2503–2514. [CrossRef]

33. Lanigan, D.T.; Mintz, S.M. Complications of surgically assisted rapid palatal expansion: Review of the literature and report of a case. *J. Oral Maxillofac. Surg.* **2002**, *60*, 104–110. [CrossRef] [PubMed]
34. Handelman, C.S.; Wang, L.; BeGole, E.A.; Haas, A.J. Nonsurgical rapid maxillary expansion in adults: Report on 47 cases using the Haas expander. *Angle Orthod.* **2000**, *70*, 129–144. [PubMed]
35. Pinto, P.X.; Mommaerts, M.Y.; Wreakes, G.; Jacobs, W.V. Immediate postexpansion changes following the use of the transpalatal distractor. *J. Oral Maxillofac. Surg.* **2001**, *59*, 994–1000. [CrossRef] [PubMed]
36. Kiliç, N.; Oktay, H. Effects of rapid maxillary expansion on nasal breathing and some noso-respiratory and breathing problems in growing children: A literature review. *Int. J. Ped. Otorhinolaryng.* **2008**, *72*, 1595–1601. [CrossRef] [PubMed]
37. Landes, C.A.; Laudemann, K.; Schübel, F.; Petruchin, O.; Mack, M.; Kopp, S.; Sader, R.A. Comparison of Tooth- and Bone-Borne Devices in Surgically Assisted Rapid Maxillary Expansion by Three-Dimensional Computed Tomography Monitoring. *J. Craniofacial Surg.* **2009**, *20*, 1132–1141. [CrossRef] [PubMed]
38. Laudemann, K.; Petruchin, O.; Mack, M.G.; Kopp, S.; Sader, R.; Landes, C.A. Evaluation of surgically assisted rapid maxillary expansion with or without pterygomaxillary disjunction based upon preoperative and post-expansion 3D computed tomography data. *Oral Maxillofac. Surg.* **2009**, *13*, 159–169. [CrossRef] [PubMed]
39. Menon, S.; Manerikar, R.; Sinha, R. Surgical Management of Transverse Maxillary Deficiency in Adults. *J. Maxillofac. Oral Surg.* **2010**, *9*, 241–246. [CrossRef]
40. Matteini, C.; Mommaerts, M.Y. Posterior transpalatal distraction with pterygoid disjunction: A short-term model study. *Am. J. Orthod. Dentofac. Orthop.* **2001**, *120*, 498–502. [CrossRef]
41. Holberg, C.; Steinhäuser, S.; Rudzki, I. Surgically assisted rapid maxillary expansion: Midfacial and cranial stress distribution. *Am. J. Orthod. Dentofac. Orthop.* **2007**, *132*, 776–782. [CrossRef]
42. Holberg, C.; Rudzki-Janson, I. Stresses at the cranial base induced by rapid maxillary expansion. *Angle Orthod.* **2006**, *76*, 543–550.
43. Lagravère, M.O.; Major, P.; Flores-Mir, C. Dental and skeletal changes following surgically assisted rapid maxillary expansion. *Int. J. Oral Maxillofac. Surg.* **2006**, *35*, 481–487. [CrossRef] [PubMed]
44. Carvalho, P.; Moura, L.B.; Trento, G.; Holzinger, D.; Gabrielli, M.A.C.; Pereira-Filho, V.A. Surgically assisted rapid maxillary expansion: A systematic review of complications. *Int. J. Oral Maxillofac. Surg.* **2020**, *49*, 325–332. [CrossRef] [PubMed]
45. Maspero, C.; Maspero, C.; Cavagnetto, D.; El Morsi, M.; Fama, A.; Farronato, M. Available Technologies, Applications and Benefits of Teleorthodontics. A Literature Review and Possible Applications during the COVID-19 Pandemic. *J. Clin. Med.* **2020**, *9*, 1891. [CrossRef] [PubMed]